α-Latrotoxin increases spontaneous and depolarization-evoked exocytosis from pancreatic islet β-cells

Amelia M. Silva[1], June Liu-Gentry[1], Adam S. Dickey[1], David W. Barnett[2] and Stanley Misler[1]

[1]*Departments of Internal Medicine and Cell Biology/Physiology, Washington University Medical Center, St Louis, MO 63110, USA*
[2]*Department of Biomedical Engineering, Saint Louis University, St Louis, MO, USA*

α-Latrotoxin (α-LT), a potent excitatory neurotoxin, increases spontaneous, as well as action potential-evoked, quantal release at nerve terminals and increases hormone release from excitable endocrine cells. We have investigated the effects of α-LT on single human, mouse and canine β-cells. In isolated and combined measurements, α-LT, at nanomolar concentrations, induces: (i) rises in cytosolic Ca^{2+}, into the micromolar range, that are dependent on extracellular Ca^{2+}; (ii) large conductance non-selective cation channels; and (iii) Ca^{2+}-dependent insulin granule exocytosis, measured as increases in membrane capacitance and quantal release of preloaded serotonin. Furthermore, at picomolar concentrations, α-LT potentiates depolarization-induced exocytosis often without evidence of inducing channel activity or increasing cytosolic Ca^{2+}. These results strongly support the hypothesis that α-LT, after binding to specific receptors, has at least two complementary modes of action on excitable cells. (i) α-LT inserts into the plasma membrane to form Ca^{2+} permeable channels and promote Ca^{2+} entry thereby triggering Ca^{2+}-dependent exocytosis in unstimulated cells. (ii) At lower concentrations, where its channel forming activity is hardly evident, α-LT augments depolarization-evoked exocytosis probably by second messenger-induced enhancement of the efficiency of the vesicle recruitment or vesicle fusion machinery. We suggest that both modes of action enhance exocytosis from a newly described highly Ca^{2+}-sensitive pool of insulin granules activated by global cytosolic Ca^{2+} concentrations in the range of ∼1 μM.

α-Latrotoxin (α-LT), a highly complex protein derived from the venom of the black widow spider, is a potent trigger of transmitter release by exocytosis of synaptic vesicles from a wide variety of resting vertebrate nerve terminals (Longenecker *et al.* 1970). It is a nearly equally potent trigger of hormone release from dense core granules of a variety of unstimulated, neuroectoderm-derived endocrine cells. These include adrenal chromaffin cells, pituitary gonadotropes and secretory terminals of the posterior pituitary (Barnett *et al.* 1996; Bittner *et al.* 1998; Tse & Tse, 1999; Hlubek *et al.* 2003; for review see Südhof, 2001). Under some conditions, α-LT appears to enhance non-vesicular release of neurotransmitter as well (Ashton *et al.* 2001). Interestingly, at tenfold lower concentrations than required for its action on resting cells, α-LT also initially enhances and subsequently blocks

depolarization-induced exocytosis at many of these sites (Longenecker *et al.* 1970; Liu & Misler, 1998).

Two distinct mechanisms of α-LT action in promoting quantal release have been proposed: (i) the ability of α-LT to form large conductance cation-selective channels (Finkelstein *et al.* 1976; Hurlbut *et al.* 1994; Barnett *et al.* 1996; Hlubek *et al.* 2000), thereby permitting Ca^{2+} entry and cytosolic Ca^{2+}-dependent exocytosis (Barnett *et al.* 1996; Liu & Misler, 1998; Bittner *et al.* 1998; Tse & Tse, 1999; Hlubek *et al.* 2003) and (ii) the ability of toxin-bound α-LT receptors to stimulate release independent of channel-forming action by enhancing recruitment of secretory granules into a pool available for release (Bittner *et al.* 1998; Liu & Misler, 1998). Three specific, high molecular weight, membrane-spanning receptors for α-LT, each containing multiple complex extracellular domains and sizeable cytoplasmic regions, have been identified at nerve terminals and secretory cells. One is a neurexin, or neuronal adhesion molecule

---

A. M. Silva, J. Liu-Gentry and A. S. Dickey contributed equally to this work

(Missler *et al.* 1998; Sudhof, 2001), another is an orphan G-protein-coupled Ca^{2+}-independent receptor for α-LT (CIRL/latrophilin) (Davletov *et al.* 1996; Krasnoperov *et al.* 1997); while the third is a tyrosine phosphatase (PTPσ) (Krasnoperov *et al.* 2002). G-protein coupling to phospholipase C, in the case of CIRL/latrophilin, and tyrosine phosphate activity, in the case of PTPσ (Rosenthal *et al.* 1990; Krasnoperov *et al.* 1997), should permit the liganded receptor to trigger intracellular signalling.

In the case of nerve terminals, considerable effort has been focused on the ability of the α-LT to enhance spontaneous quantal release (miniature endplate potential frequency) in the absence of extracellular calcium (Ca_o^{2+}) or an accompanying rise in intracellular calcium (Ca_i^{2+}), especially as this mode of toxin action produces, over time, as much quantal release as is seen with toxin in the presence of Ca_o^{2+} (Misler & Hurlbut, 1979; Meldolesi *et al.* 1984; Tsang *et al.* 2000). This 'Ca^{2+}-independent release' supports the notion that an action of α-LT, apart from its capacity to form channels, contributes substantially to its ability to sustain massive increases in spontaneous quantal release. In contrast, in unstimulated but excitable endocrine cells, the majority of recent evidence argues strongly that the bulk of massive toxin-induced exocytosis results from Ca^{2+} entry through non-selective cation channels, formed by bound toxin, followed by the accumulation of cytosolic Ca^{2+} to levels similar to those that trigger sustained exocytosis from permeabilized or dialysed cells (Liu & Misler, 1998; Tse & Tse, 1999; Hlubek *et al.* 2003). However, one apparent exception among endocrine cells is the endoderm-derived, insulin-secreting pancreatic β-cell. Though β-cells have ample α-LT receptors and display similar depolarization-induced, Ca^{2+} entry-dependent exocytosis as adrenal chromaffin cells, Lang *et al.* (1998) have reported that application of α-LT in the presence of substimulatory concentrations of glucose produces small increases in insulin release both in the presence or in the absence of Ca_o^{2+} that are not associated with a rise in cytosolic Ca^{2+} or cell depolarization. These results suggest that, as at nerve terminals, in β-cells α-LT might enhance exocytosis in a manner independent of its channel-forming or Ca^{2+} entry-enhancing activities. However, these results are in stark contrast to the results of our own preliminary studies of α-LT on intact human islets where we found that brief addition of α-LT to human islets incubated in the presence of a physiological saline solution produced several fold greater insulin release than after addition of toxin in the presence of very low Ca^{2+} (no added Ca^{2+} PSS $+1$ mM EGTA; Supplemental Materials).

In this study we have investigated (i) whether α-LT can enhance both resting (or spontaneous) quantal release and depolarization-evoked quantal release from β-cells and (ii) how the proposed mechanisms of 'channel formation/Ca^{2+} entry' and 'ranule recruitment' contribute independently and as well as in a complementary manner to enhance these two modes of quantal release. To avoid possible cytolytic effects of the toxin (e.g. Okamoto *et al.* 1971) that might be difficult to detect in whole islets, we studied the effects of toxin on single-cell exocytosis from short-term cultured human, mouse and canine islet cells whose intactness could be directly visualized. Specifically, we performed real-time single-cell electrophysiological and electrochemical assays of exocytosis, namely membrane capacitance and amperometry, as well as Ca^{2+}-imaging experiments closely comparable to those we previously performed on adrenal chromaffin cells (Liu & Misler, 1998), using batches of toxin that we found to be highly active on chromaffin cells. As was the case with adrenal chromaffin cells and secretory terminals of the posterior pituitary (Liu & Misler, 1998; Hlubek *et al.* 2003), quantal release from resting cells was massively augmented by α-LT, but only (i) in the presence of sufficient $[Ca^{2+}]_o$, (ii) after inducing Ca^{2+}-permeable cation channels and (iii) after raising cytosolic $[Ca^{2+}]$ to levels that trigger exocytosis in permeabilized or internally dialysed β-cells. Hence, the 'channel formation/Ca^{2+} entry' mechanism appears to be essential for the toxin's secretagogue action on resting β-cells. However, as in chromaffin cells, lower concentrations of α-LT, which produce little or no channel activity and/or little or no increase in baseline $[Ca^{2+}]_i$ nevertheless enhance a slow, asynchronous component of depolarization-induced exocytosis, strongly suggesting an additional mechanism of toxin action, namely 'insulin granule recruitment'. These complementary mechanisms are likely to interact in a positive fashion: (i) granule recruitment bolstering the channel-forming action on resting cells, given sufficient Ca^{2+} entry to support exocytosis; and (ii) channel-forming activity, when present, augmenting granule recruitment by raising cytosolic Ca^{2+} concentration.

Some of these results have previously been reported in abstract form (Liu-Gentry *et al.* 2004).

Methods

Preparation of islets and single islet cells

Cells from human, canine and murine islets were used in this study to take advantage of their special properties and to facilitate comparison with other studies. Human islet cells are the most relevant to medical physiology. Canine islet cells display electrophysiological and secretory patterns similar to human and, on a cell for cell basis, are more potent secretors as single cells, although they load poorly with membrane-permeant fluorescent indicator dyes. Murine islet cells are more generally available, have been used in prior studies of toxin (Lang *et al.* 1998) and are genetically most manipulable, hence making them likely candidates for future, more molecularly orientated studies.

Canine and human islets of Langerhans were the gift of the Islet Transplantation Laboratory of

Washington University. Canine pancreata were removed from mongrel dogs of either sex, anaesthetized with sodium pentobarbital, following protocols approved by the Animal Studies Committee of Washington University Medical Center. Human pancreata were removed from life-supported human cadavers, during organ harvesting for renal, liver or cardiac transplantation, following protocols approved by the Human Studies Committee of our institution. Both human and canine minced pancreatic tissue were digested with collagenase and islets were separated on a Ficoll gradient according to previously developed protocols (Ricordi *et al.* 1988). Mouse islets were the gift of the laboratory of Dr Kenneth Polonsky (Dept Internal Medicine, Washington University Medical Center, St Louis, MO, USA). They were prepared according to a modified version of the protocol of Lacy & Kostianovsky (1967) and approved by the Animal Studies Committee of Washington University Medical Center.

Freshly isolated islets were suspended in serum-enriched, Hepes-buffered CMRL-1066 culture medium containing 5 mM glucose (Gibco, Grand Island, NY, USA) and then maintained for up to 10 days at (17–20°C), prior to their dispersion to single cells. Combined enzymatic plus mechanical dispersions were performed in a test tube in either of two ways. (i) Islets were incubated for 1–3 min in Versene 1 : 5000 (Gibco BRL, Grand Island, NY, USA), and then exposed to dispase (0.33 mg ml^{-1}, Boehringer Mannheim GmbH, Germany) in the presence of gentle stirring. (ii) Islets were briefly incubated at 30°C in trypsin-EDTA 1X (Sigma, St Louis, MO, USA) accompanied by mechanical disruption. Islet cells were plated on glass coverslips and then incubated in a 5% CO_2–95% air environment at 37°C for up to 5 days prior to their use in these experiments.

Conditions for single cell recording

Two to 5 days after islet dispersion, single-cell recordings were made at 30–33°C in a standard Hepes-buffered physiological saline solution (PSS) containing (mM): NaCl 140, KCl 5.5, $CaCl_2$ 2, $MgCl_2$ 1.0, glucose 2 and Hepes 20; titrated to pH 7.3 with NaOH. Throughout the text this solution will be referred to as '2 mM Ca^{2+} PSS'. The glucose concentration or ionic composition of the bath was altered by iso-osmotic substitution of a portion of the NaCl. In experiments where exocytosis was directly measured, forskolin (10 μM) or isobutylmethylxanthine (500 μM) was added to increase the efficiency of coupling of depolarization to secretion (Barnett *et al.* 1994).

Recording techniques and data analysis

Techniques used for recording of electrophysiological and spectrofluorometric data were identical to those we have previously described (Liu & Misler, 1998). Electro-physiological recordings were made using the perforated patch variant of whole cell recording. The recording patch pipettes were filled with a standard high-K^+ internal solution (K^+-IS) for current clamp and ion selectivity experiments or a high-Cs^+ internal solution (Cs^+-IS) for experiments in which increases in membrane capacitance were measured and related to Ca^{2+} entry. K^+-IS contained (mM): KCl 63.7, K_2SO_4 28.35, sucrose 47.2, NaCl 11.8, $MgCl_2$ 1 and Hepes 20; titrated to pH 7.3 with KOH. Cs^+-IS resembled K^+-IS except that KCl was replaced by CsCl and K_2SO_4 was replaced by Cs_2SO_4. After filling the tip of the pipette by capillary, 3–5 μl of a nystatin-containing solution (250 μg ml^{-1}) was injected into the pipette just proximal to its tip. For voltage-clamp experiments the membrane potential was maintained at a holding potential (V_h) of −70 mV throughout the experiment and sinusoidal or square pulse excitation was imposed as needed. For current-clamp experiments a small holding current was occasionally used to maintain a resting membrane potential of −65 mV. Cells chosen for extended study were the largest single cells seen (> 10–12 μm in diameter) and had a baseline capacitance of > 5.5 pF. The use of the latter selection criteria increased the probability that the cells examined were β-cells (e.g. Pipeleers & Van de Winkel, 1987; Gopel *et al.* 1999).

The membrane capacitance (C_m) of the patch-clamped cell was estimated along the with (i) the access resistance (R_a) between the pipette filling solution and the interior of the cell and (ii) the membrane resistance (R_m) using a software-based, dual frequency lock-in detector (LID) developed as a set of extensions (XOP modules) of the numerical/graphics package Igor (Wavemetrics Inc., Lake Oswego, OR, USA) and run on a Macintosh Quadra-650 (Apple Inc., Cupertino, CA, USA) (Barnett & Misler, 1997). A double sinusoidal stimulus (10 mV peak-to-peak at 400 and 800 Hz) was applied to an EPC-9 patch-clamp amplifier (Heka Electronic, Lambrecht, Germany) held at a DC potential of −70 mV. The resultant membrane current signal at each frequency, which is phase shifted from the input voltage signal, was digitized by a 16-bit A/D converter card (ITC-16, Instrutech, Syosset, NY, USA) and fed into the LID, which decomposed it into real (or 'in-phase') and imaginary (or 'quadrature') components of the admittance. Based on these four measurements, a non-linear weighted least-squares algorithm is used to estimate and display in real time the values of R_m, C_m and R_a. In this configuration the DC membrane current (I_m) at −70 mV, estimated by averaging the sampled current over the period of the lower frequency sine wave (i.e. 2.5 ms), is also displayed to track background channel activity. By interrupting the sinusoidal excitation with square steps of depolarization it is possible to examine depolarization-induced exocytosis as well. This software runs the spectrofluorometer, used for ratiometric monitoring of cytosolic Ca^{2+} via a Ca^{2+}-sensitive dye, by

triggering the monochromator (Polychrome II; Till Photonics Photometrics System, Applied Scientific Instruments Inc., Eugene, OR, USA) and displaying the output of a photomultiplier tube.

Amperometry

Four to 16 h prior to recording, serotonin (5-hydroxytryptamine, 5-HT) and 5-hydroxytryptophan were added to the culture media at final concentrations of 1 mM (Smith *et al.* 1995). Five to 20 min prior to recording, the cells were transferred to the recording chamber and perifused for at least 30 s with PSS. Recordings were performed with polypropylene-insulated carbon fibre electrodes (CFEs) (Zhou & Misler, 1996) touching the cell surface. The CFEs were held at +650 mV using an EPC-7 amplifier (Heka Electronic). Amperometric data, filtered at 300 Hz using an 8-pole Bessel filter (Frequency Devices Haverhill, MA, USA), were acquired simultaneously with membrane current or membrane voltage data using the software package which runs the digital LID. Amperometric events were reviewed and tabulated with an interactive Igor-based program in use in our lab. The criteria for scoring an amperometric event were (i) an amplitude of at least 1 pA ($\sim$3 times the peak-to-peak background noise of acceptable recordings) and (ii) a half-height duration of at least 2 ms (Zhou & Misler, 1996).

Ratiometric monitoring of cytosolic Ca^{2+}

Cytosolic Ca^{2+} concentration was estimated from ratiometric measurements made on cells loaded with membrane-permeant, esterified derivatives (acetoxymethly ester, AM) of Fura-2 or Fura-4F (Molecular Probes, Eugene, OR, USA). Cells were incubated in Hepes-buffered Dulbecco's modified Eagle's medium (DMEM) containing 5 μM Fura-2AM or Fura-4FAM for 20–30 min at room temperature, and then washed with DMEM + 10% fetal bovine serum for 20–30 min to allow de-esterification of the dye. This provided uniform loading of the cytoplasm and fluorescence emission at levels > 5-fold higher than the autofluorescence. Cells were then transferred to the stage of a Leitz epifluorescence microscope, equipped for dual wavelength (340 and 380 nm) excitation and appropriate throughput of fluorescence emission at 510 nm, for spectrofluorometric monitoring either by (i) single-cell photon counting, coupled with our data Igor-based data acquisition system discussed above, or (ii) multicell fluorescence imaging using an intensified CCD camera, coupled to a frame grabber board capable of digitizing the paired emission images. Either approach enabled analysis of 'ratio' images for designated regions of the field.

For each designated optical region of interest, ratiometric data were converted to a running estimate of $[Ca^{2+}]_i$, using a standard equation:

$$[Ca^{2+}]_i = K_d (R - R_{min})/(R_{max} - R) \times (F_{380,max}/F_{380,min})$$

where $K_d = 224$ nM for Fura-2 and 770 nM for Fura-4F, respectively, and R_{max} and $F_{380,max}$ and R_{min} and $F_{380,min}$ were obtained sequentially after adding 5 μM ionomycin and then at least 5 mM EGTA to the bath solution (Grynkiewicz *et al.* 1985).

Materials

High-potency α-latrotoxin was obtained from Alomone (Jerusalem, Israel) or from Dr Alexandre Petrenko (New York University Medical Center). Screening experiments presented in Figs 1–3 were performed with commercially purified toxin, while more detailed experiments with combined assays utilized aliquots of somewhat more potent toxin obtain from Dr Petrenko. Salts and other chemicals, when not mentioned, were from Sigma.

Statistical significance was determined by analysis of variance (ANOVA). Results are presented as means ± s.d.

Results

Nanomolar concentrations of α-LT induce large rises in $[Ca^{2+}]_i$, large conductance channels and Ca^{2+}_o-dependent exocytosis in single pancreatic islet cells

Figures 1–3 present the three key observations of this study. First, Fig. 1*A* and *B* shows that in human islet cells, including those with clear glucose responsiveness, applications of α-LT at nanomolar concentrations increases $[Ca^{2+}]_i$ from an estimated baseline of $\sim$200 nM into the range of many hundreds of nanomolar. These rises are comparable in peak amplitude to those produced by a high-K^+ stimulus (KCl, 30 mM) and are dependent on the presence of adequate $[Ca^{2+}]_o$. These responses occur without evidence of significant cell swelling, blebbing or nuclear accentuation. $[Ca^{2+}]_i$ is reversibly reduced to near baseline within 2–3 min of admission to the bath of a no added Ca^{2+}/EGTA PSS (a PSS containing no added Ca^{2+} and 1 mM EGTA). In Fig. 1*B*, note that occasional brief spike-like increases in $[Ca^{2+}]_i$ occur in a minority of cells in the presence of α-LT concentrations as low as 1 nM.

The traces in Fig. 1*C* examine more closely the dose-dependence of α-LT action. They show that application of 1 nM α-LT to human islets cells bathed in PSS produces a spike-like increase in estimated $[Ca^{2+}]_i$ in four out of 22 KCl-responsive cells (average maximum $[Ca^{2+}]_i$, 455 ± 53 nM). In contrast, application of 5 nM α-LT produces a response in 21 out of 22 KCl-responsive

cells, with 11 cells responding with a spike-like increase in estimated $[Ca^{2+}]_i$ (maximum $[Ca^{2+}]_i$, 567 ± 70 nM) and 10 responding with a sustained increase in estimated $[Ca^{2+}]_i$ (maximum $[Ca^{2+}]_i$, 804 ± 80 nM). Finally, application of 10 nM α-LT produces a sustained increase in estimated Ca_i^{2+} in six out of six KCl-responsive cells (maximum $[Ca^{2+}]_i$, 1380 ± 330 nM).

The traces in Fig. 1D demonstrate that α-LT remains effective on human islet cells even when briefly applied, and washed out with a very low $[Ca^{2+}]_o$ PSS (no added Ca^{2+}/EGTA PSS), provided adequate Ca_o^{2+} is later added. Comparing the traces in Fig. 1D with those in Fig. 1A, note that under the latter condition the toxin is equally potent as when it is initially applied in adequate $[Ca^{2+}]_o$. This suggests that binding of α-LT is relatively rapid (occurring within minutes) and not highly dependent on extracellular Ca^{2+}.

Using mouse islets cells that respond more uniformly and vigorously to glucose, the traces in Fig. 1E and F show that the toxin acts potently in the presence of both diazoxide (250 μM), an opener of ATP-dependent K^+ channels that hyperpolarizes β-cells, and nifedipine (50 μM), a potent inhibitor of L-type voltage-dependent Ca^{2+} channels (VDCC), though either agent alone is sufficient to block a glucose-induced rise in $[Ca^{2+}]_i$. This suggests that α-LT is operating to enhance $[Ca^{2+}]_i$ in a manner independent of the principal pathway of stimulus–depolarization coupling, namely glucose metabolism leading to closure of K^+(ATP) channels leading to cell depolarization leading to opening of VDCCs.
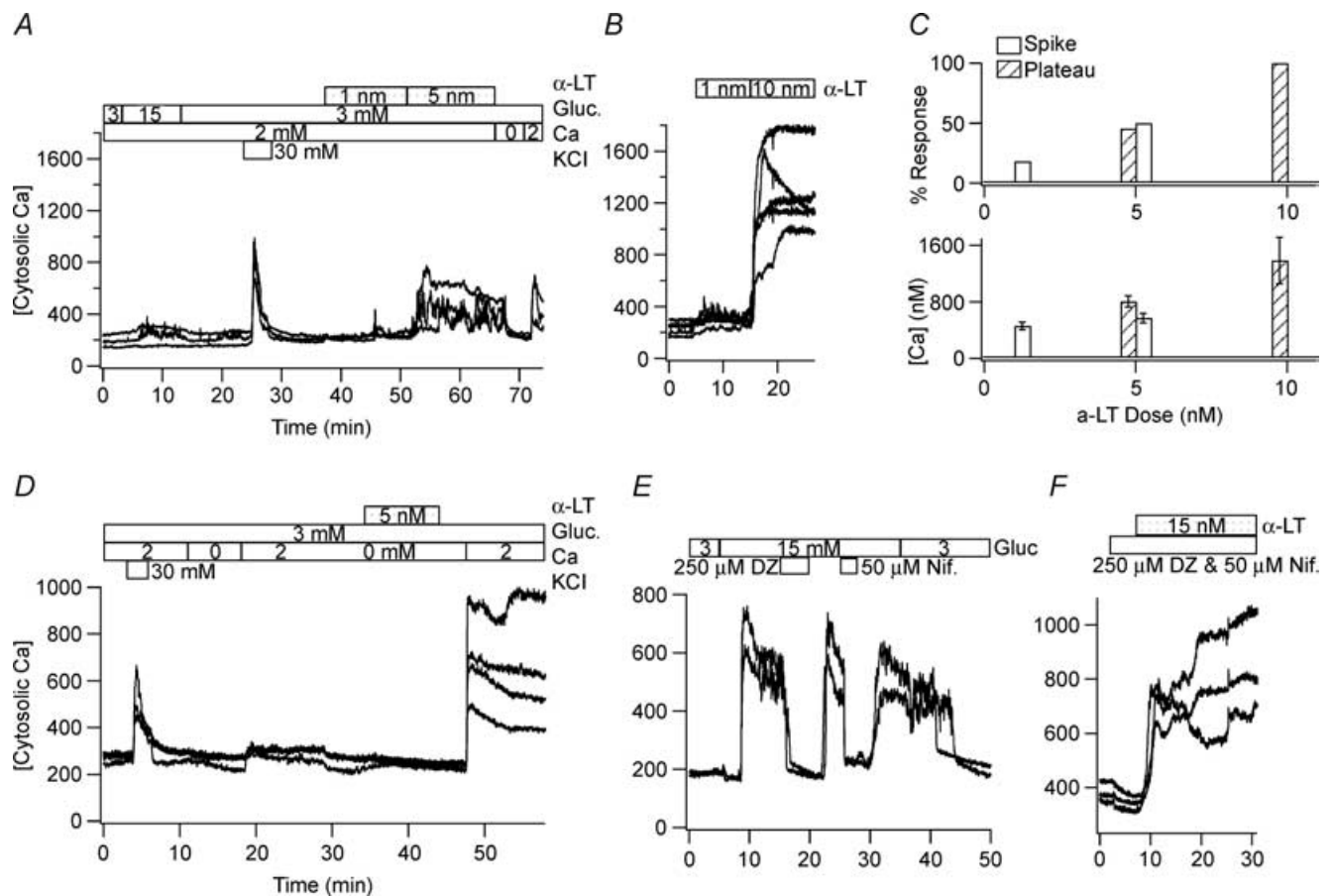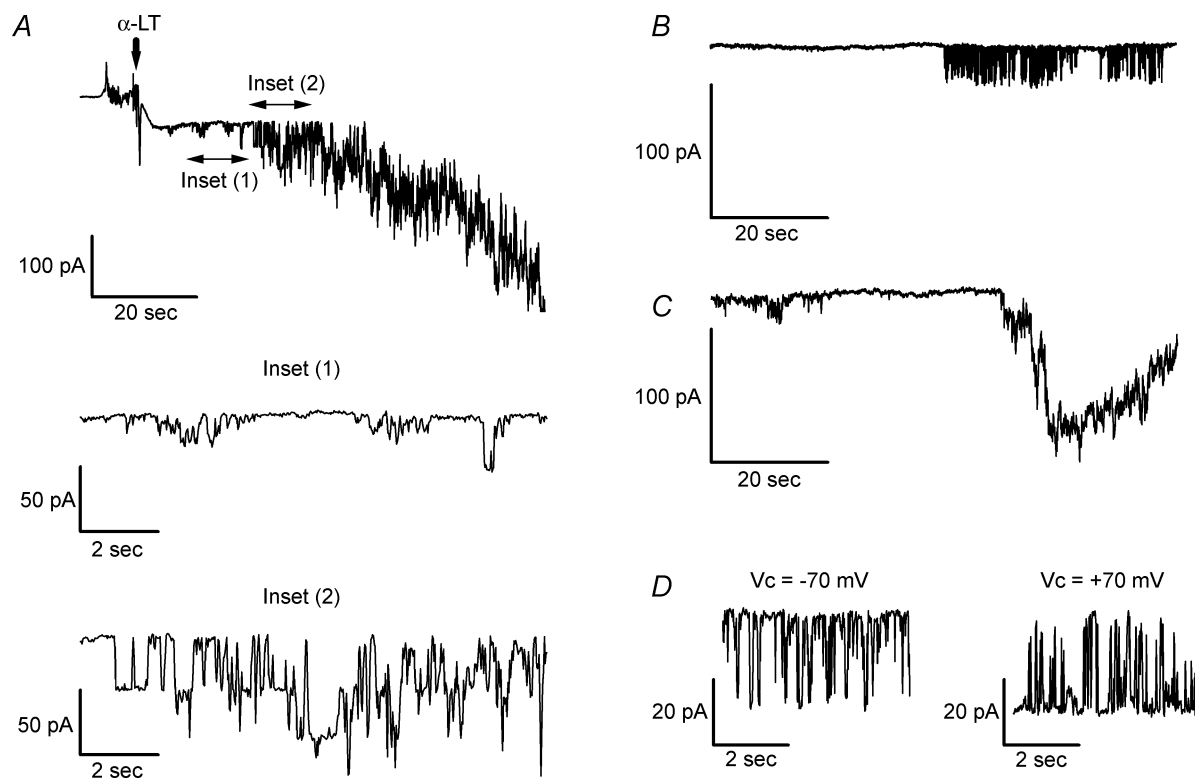

Figure 1. Nanomolar concentrations of α-LT cause large changes in $[Ca^{2+}]_i$ of human and mouse islet cells that are dependent on the presence of an adequate $[Ca^{2+}]_o$
A and *B*, 5 nM and 10 nM α-LT, respectively, raise the estimated $[Ca^{2+}]_i$ in representative glucose- and KCl-responsive human islet cells from baseline level of ~200 nM to a maximum level of ~450 nM and ~800 nM, respectively, while 1 nM α-LT generates brief spikes in a minority of cells. *C*, top histograms show the percentage of human cells responding to α-LT with an increase in $[Ca^{2+}]_i$ found by those displaying transient spikes (filled bar) *versus* a more sustained plateau (striped bar). *C*, bottom histograms show the corresponding average of maximum $[Ca^{2+}]_i \pm$ s.d. of the responding cells. *D*, α-LT binds equally well in the absence of Ca_o^{2+}. *E* and *F*, the combination of 250 μM diazoxide (an opener of ATP-dependent K^+ channels), which hyperpolarizes β-cells, and 50 μM nifedipine (a blocker of L-type voltage-dependent Ca^{2+} channels), which blocks depolarization-induced electrical activity, does not militate the effect of α-LT on $[Ca^{2+}]_i$ while either drug alone blocks a glucose-induced rise in $[Ca^{2+}]_i$.

Second, Fig. 2 shows that in large diameter human islet cells, likely to be β-cells, nanomolar concentrations of α-LT induce large conductance membrane channels, as monitored in the perforated patch variant of whole-cell voltage-clamp recording at near the cells' resting membrane potentials. In Fig. 2A note that after application of 2–5 nm α-LT at -70 mV, human islet cells display inward unitary current openings ranging in amplitude from 10 pA, on first appearance (see inset 1 for a magnified view of this), to > 30 pA when they occur at greater frequency (see inset 2). Alternatively, initial openings may occur in discrete bursts (see Fig. 2B) or develop over time in a superposed manner to give rise to brief (10–30-s duration) spikes of membrane current greater than 100 pA in magnitude (see Fig. 2C). As seen in Fig. 2D, toxin-induced currents reverse direction and become outward at clamping potentials positive to 0 mV (compare current traces recorded at -70 mV and $+70$ mV). After application of 7–10 nm α-LT, membrane current often approached 1 nA (data not shown). The complex features of these currents and their intimate

relationship to exocytosis will constitute the majority of the remainder of this paper.

Third, Fig. 3, in which amperometric current (I_{amp}) is monitored over minutes, shows that nanomolar concentrations of α-LT induce Ca^{2+}-dependent exocytosis, measured as developing barrages of quanta (discrete spikes) of 5-HT released onto the surface of a human islet cell and oxidized at the surface of a carbon fibre electrode. Figure 3A shows a clear example of a barrage of amperometric spikes (AS) beginning seconds after a puff of 10 nm α-LT onto a cell bathed in 2 mm Ca^{2+} PSS. The discrete nature of this barrage contrasts with the effects of poking the cell with the carbon fibre electrode, a situation in which individual spikes overlay a 'hump' of increased amperometric activity. The quanta of 5-HT represent, on average, a total charge transfer of up to 400 fC. Assuming the transfer of four electrons per molecule of 5-HT oxidized (Bruns & Jahn, 1995), on average each amperometric event corresponds to the synchronous oxidation of 6×10^5 molecules of 5-HT per release event ($1e^- = 1.6 \times 10^{-19}$ C). This range of

Figure 2. Nanomolar concentrations of α-LT induce large conductance membrane channels
Traces were recorded from large diameter human islet cells in response to application of 2–5 nm α-LT, using the perforated patch variant of whole-cell voltage-clamp recording. A, addition of α-LT at a clamping potential (V_c) of -70 mV leads to discrete current openings that sum to yield a net inward current exceeding 300 pA. Inset 1, which magnifies a 12-s segment of the above trace, starting 9 s after addition of α-LT, shows that current jumps are $\sim$10 pA in amplitude. Inset 2, which magnifies another 12-s segment starting 21 s after α-LT openings, shows that current jumps are > 30 pA in amplitude. B, current openings sometimes occur in discrete bursts. C, current openings sometimes sum to produce a large transient inward current of similar duration (as the brief Ca^{2+} spikes seen in Fig. 1). D, currents are equal in amplitude, though opposite in direction, at V_c of -70 mV and of $+70$ mV.

molecular release would be expected for exocytosis from a 200- to 300-nm diameter granule well loaded with 5-HT (Zhou & Misler, 1996). Hence, 5-HT, which is specifically concentrated into insulin granules of β-cells as a 'false transmitter' during exogenous loading by bath incubation, serves as an easily assayed surrogate marker for granular insulin release. This suggests that 5-HT released by toxin is released from intracellular packets rather than simply diffusing out of the cytoplasm through a discrete pore or non-specific membrane disruption caused by α-LT.

In contrast, as seen in Fig. 3*B*, human islet cells bathed in no added Ca^{2+}/EGTA PSS display no amperometric spikes after a puff of 10 nM α-LT. However, a subsequent application, by puffer pipette, of PSS containing 10 mM Ca^{2+} in the vicinity of the cell leads to the abrupt onset of quantal spikes.

Figure 3*C* and *D* displays the cumulative total (Σ) of amperometric spike events (ΣAS) as a function of time after addition of α-LT for experiments of the same type as shown in Fig. 3*A* and *B*, respectively. In Fig. 3*C*, note that in the presence of adequate $[Ca^{2+}]_o$, application of 50 μM nifedipine (Fig. 3*C*, ○), has no discernable effect on toxin-induced amperometric barrage. The striking

similarities of Ca^{2+} dependence, time of onset and pharmacology of toxin-induced rise in $[Ca^{2+}]_i$ and quantal release of 5-HT suggests that the former may underlie the latter.

Relationship of α-LT-induced channel activity to exocytosis and rise in cytosolic Ca^{2+} in patch-clamped β-cells

In single patch-clamped canine islet cells, selected for their large size (diameter, > 10–12 μm) and their ability to exocytose in response to repetitive depolarization (ten 200-ms pulses to +10 mV, from V_h of − 70 mV, applied at 1 Hz), we examined the temporal relationship of toxin-induced channel activity to exocytosis (membrane capacitance increase or amperometric spike activity) in the presence of bath solutions with various Ca^{2+}_o concentrations. In cells also loaded with the fluorescent Ca^{2+} indicator Fura-2 we examined the temporal relation of the rise in $[Ca^{2+}]_i$ to channel activity and exocytosis.

In Fig. 4, large diameter, depolarization-responsive cells, patch clamped with Cs^+-IS pipette and subjected to continuous small-signal (10 mV peak-to-peak) dual-sinusoidal voltage excitation about a mean V_m of
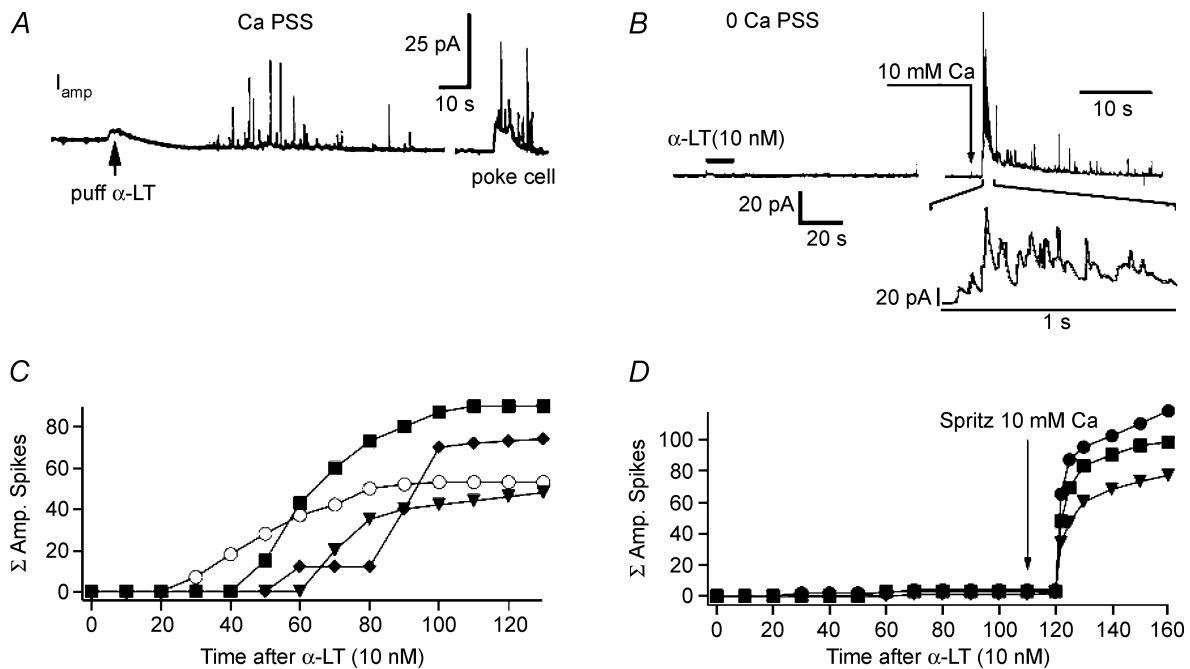
Figure 3. Nanomolar concentrations of α-LT induce Ca^{2+}-dependent exocytosis
A, application of 10 nM α-LT, by puffer pipette, in the vicinity of a human islet cell bathed in 2 mM Ca^{2+} PSS produces a barrage of discrete spikes in the amperometric current trace I_{amp}. This response is distinct from the 'dome + spike' pattern produced by a subsequent brief 'poke' of the cell with a carbon fibre electrode. *B*, in contrast shows that 10 nM α-LT applied by puffer pipette in the vicinity of a human islet cell bathed in no added Ca^{2+}/EGTA PSS produces no spikes in I_{amp}, until Ca^{2+} is later added to the bath via close-range application of 10 mM Ca^{2+} PSS from a second puffer pipette. *C* and *D*, display, for identical experiments of the types illustrated in *A* and *B*, respectively, the cumulative total amperometric spike events (ΣAS) *versus* time after addition of α-LT. *C*, in some experiments 50 μM nifedipine (○)?was added to block endogenous voltage-dependent Ca^{2+} channels.

-70 mV, were treated with 5 nM α-LT (by puffer pipette application) in the presence of 2 mM Ca^{2+} PSS or no added Ca^{2+}/EGTA PSS. In the majority of cells tested in either ionic condition (10/13 in 2 mM Ca^{2+} PSS *versus* 5/7 in no added Ca^{2+}/EGTA PSS) addition of α-LT induced vigorous inward current channel activity that commenced within 120 s after application of the toxin and continued to develop for at least 60–120 s thereafter. Under both conditions, at 300 s after α-LT application, total toxin-induced inward current was indistinguishable under the two ionic conditions (-365 ± 325 pA in 2 mM Ca^{2+} PSS *versus* -430 ± 300 pA in no added Ca^{2+}/EGTA PSS). However, under divergent ionic conditions the effects of toxin on membrane capacitance were quite different (as shown in sample traces in Fig. 4*A* and summarized data in Fig. 4*B*).

Of the 10 'toxin-responsive' cells examined in 2 mM Ca^{2+} PSS, seven cells showed sustained increase in C_m during the build-up of channel activity, while three cells (e.g. Fig. 4*A*, top left trace) showed an initial progressive increase in C_m followed by an abrupt drop. Channel activity in the 2 mM Ca^{2+} PSS consisted of 'flickery' jumps between several current levels. In addition, in 10/10 of the highly 'toxin-responsive' cells examined in 2 mM Ca^{2+} PSS, repetitive depolarization during toxin-induced channel activity failed to show steps in C_m. In contrast, in the presence of no added Ca^{2+}/EGTA PSS, little or no increase in C_m occurred in any of the cells (Fig. 4*A*, top right panel) despite the total inward membrane current growing by prolonged, uniform steps to values comparable to those seen in 2 mM Ca^{2+} PSS.

Comparison of capacitance increases produced by α-LT in 2 mM Ca^{2+} PSS *versus* no added Ca^{2+}/EGTA PSS strongly suggested that the link between toxin-induced channel activity and exocytosis was likely to be entry of Ca^{2+} into the cytosol via Ca^{2+}-permeable toxin-induced ion channels. This hypothesis was further tested in experiments detailed in Figs 5–7.

Figure 5 shows two direct tests of the hypothesis of Ca^{2+} entry, via toxin-induced channels, using patch-clamped human β-cells previously loaded with Fura-2 and tested in modified PSS. In Fig. 5*A*, in the presence of 90 mM Ca^{2+} PSS (solution compounded by isosmotically replacing all of the NaCl by $CaCl_2$), C_m, $[Ca^{2+}]_i$ and I_m were monitored simultaneously. In this, and in three other similar experiments, we noted that application of α-LT initially produced current jumps of smaller amplitude (~ 8 pA at -70 mV) and of longer duration than in standard 2 mM Ca^{2+} PSS (see magnification in Fig. 5, inset 1). The opening of only one channel for 50–60% of the elapsed time detectably raised $[Ca^{2+}]_i$. Later, the composite opening of two to three channels, producing an inward current of -20 pA, raised $[Ca^{2+}]_i$ to > 600 nM, and initiated a progressive rise in C_m.

In contrast, Fig. 5*B* displays typical results of a set of three different experiments where I_{amp}, $[Ca^{2+}]_i$ and I_m were monitored simultaneously after application of α-LT in the presence of no added Ca^{2+}/EGTA PSS and after local pulse application of 90 mM Ca^{2+} PSS at $t = \sim 105$ s (i.e. during the gap in the $[Ca^{2+}]_i$ trace). Here, identical application of α-LT as performed in Fig. 5*A* produced long stepwise increases in current (see magnification
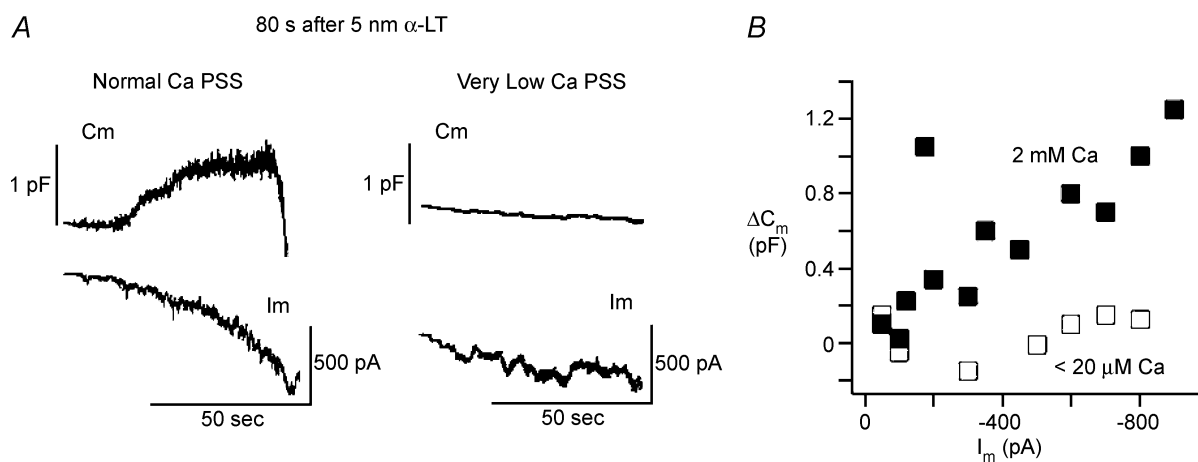
Figure 4. Relationship of α-LT-induced channel activity to exocytosis in physiological and in very low $[Ca^{2+}]_o$

*A*, close application of 5 nM α-LT (left traces) in the vicinity of a canine islet cell bathed in 2 mM Ca^{2+} PSS, induces a progressively increasing inward I_m followed by a large increase in C_m once the induced inward current I_m exceeds -100 to -150 pA. In contrast, right-hand traces demonstrate that a similar puff of α-LT in the vicinity of a canine islet cell bathed in no added Ca^{2+}/EGTA PSS (< 20 μM free Ca^{2+}) produces little or no increase in C_m despite stepwise increase in I_m to -300 to -350 pA. *B*, demonstrates that in 2 mM Ca^{2+} PSS (■) the total change in membrane capacitance (ΔC_m) is proportional to the toxin-induced inward membrane current I_m; whereas, in no added Ca^{2+}/EGTA PSS (□), ΔC_m is barely detectable despite similarly wide range of increases in I_m.

in Fig. 5, inset 2) that rapidly superposed. Though the total membrane current approached −800 pA, no rise in $[Ca^{2+}]_i$ or amperometric spike events occurred. However, within 5 s after a 5-s application by puffer pipette of 90 mM Ca^{2+} PSS in the close vicinity of the cell, inward membrane current drastically decreased, $[Ca^{2+}]_i$ rose to levels that saturated the Fura-2 signal, and an intense burst of amperometric spike activity occurred.

We validated the concordance of our assays of toxin-induced exocytosis by the approaches shown in Fig. 6. Figure 6*A* compares the time course of capacitance increase with that of the amperometric discharge and demonstrates that at least early in toxin-induced exocytosis both assays monitor release from the same store of

fusion-competent intracellular organelles. Note that between 58 and 75 s after application of α-LT, the rise in C_m and the development of amperometric activity are most intense, while for the remainder of the recording C_m decreases as the amperometric discharge slows. Figure 6*B* shows that during the initial phase of the discharge, the running sum of amperometric spike events, ΣAS (bottom trace), closely parallels the developing increase in C_m, $\Sigma \Delta C_m$ (top trace, ●). To further analyse the time course of these recordings, we made the following assumptions. (i) Each AS corresponds to an exocytotic event that increases C_m by 1.5–2.0 fF. (ii) The efficiency of capture of an exocytotic event by the carbon fibre electrode remains constant over the entire discharge. Based
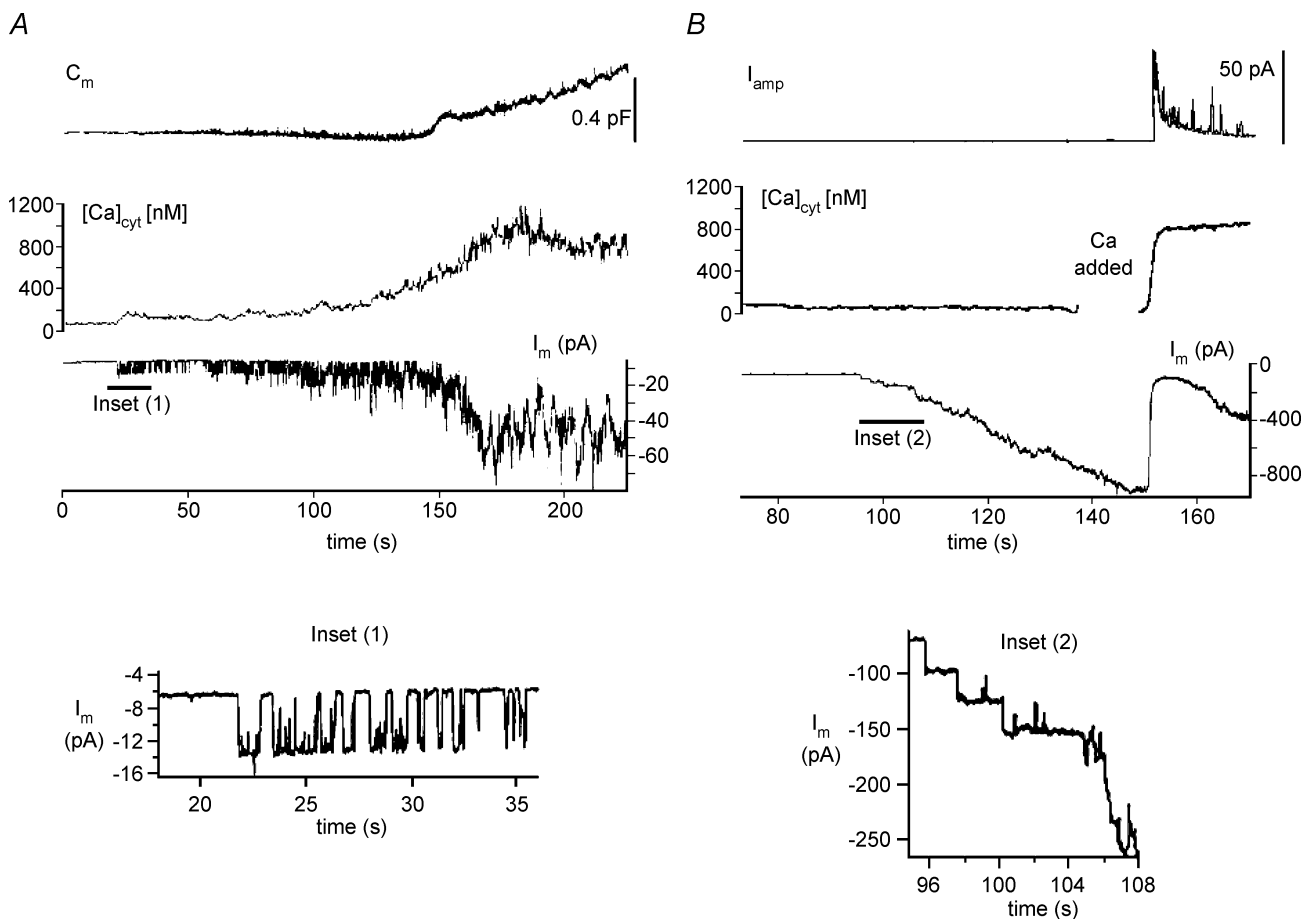

Figure 5. α-LT-induced exocytosis is dependent on Ca^{2+} entry in human β-cells

A, time courses of changes in C_m, $[Ca^{2+}]_i$ and whole-cell currents (I_m), recorded simultaneously, in a human β-cell bathed in 90 mM Ca^{2+} PSS, beginning 55 s after application of 5 nM α-LT. Inset 1, note that the increase in I_m begins as large steps of inward current (7–8 pA). Thereafter, $[Ca^{2+}]_i$ rises, first slowly and then more rapidly, as I_m increases. After $[Ca^{2+}]_i$ rises to > 600 nM, C_m begins to rise along a complex time course. *B*, combined measurements of the time courses of development of I_{amp}, $[Ca^{2+}]_i$ and I_m in a human β-cell bathed in no added Ca^{2+}/EGTA PSS, beginning 40 s after application of 5 nM α-LT. Inset 2, under these conditions, the increase in I_m begins as larger (~25 pA) and more sustained inward current steps than in inset 1. Also, despite the increase in I_m to > −600 pA, neither a rise in $[Ca^{2+}]_i$ nor a development in I_{amp} is seen until a puff of 90 mM Ca^{2+} PSS is applied to a region of the bath near the cell. The interruption in the continuity of the $[Ca^{2+}]_i$ trace indicates the time when the shutter of the photomultiplier tube of the imaging setup was closed and the recording chamber was illuminated briefly to allow the application of Ca^{2+}.

on these assumptions, Fig. 6*B* demonstrates that over the initial phase of the discharge, ΔC_m estimated from the AS discharge (top trace, ○) is virtually superimposable on ΔC_m actually measured, assuming a 30% efficiency of capture of an amperometric event. The subsequent splay between the observed and estimated ΔC_m probably represents endocytosis. Similar results were observed in another experiment where the efficiency of capture of an amperometric event was 12–15%. The flatness of the background I_{amp} trace from which the spike events arise suggests that non-quantal release of 5-HT contributes little to the transmitter release evoked by the toxin.

Figure 6*C* relates toxin-induced exocytosis, measured by amperometry, to toxin-induced membrane depolarization and electrical activity as recorded in the current-clamp mode. Note that 112 s after application of α-LT in 2 mM

glucose PSS, the cell, which previously maintained a stable resting potential near −65 mV, depolarized and then fired an intense train of action potentials, at the end of which a brief burst of spikes is seen in the I_{amp} trace. Subsequently, the membrane further depolarized to a maintained plateau of ∼0 mV, and an intense barrage of amperometric spikes lasting tens of seconds was seen. A check of membrane conductance (G_m), calculated from the hyperpolarization caused by a brief injection of −5 pA of current (not shown), revealed that during the extended plateau depolarization to near 0 mV, G_m increased by 10-fold (range, 7- to 12-fold in four cells) as compared with an interval prior to toxin application. The effect of the toxin on G_m is opposite to that caused by application of a standard depolarizing secretagogue for β-cells. For example, raising bath glucose concentration
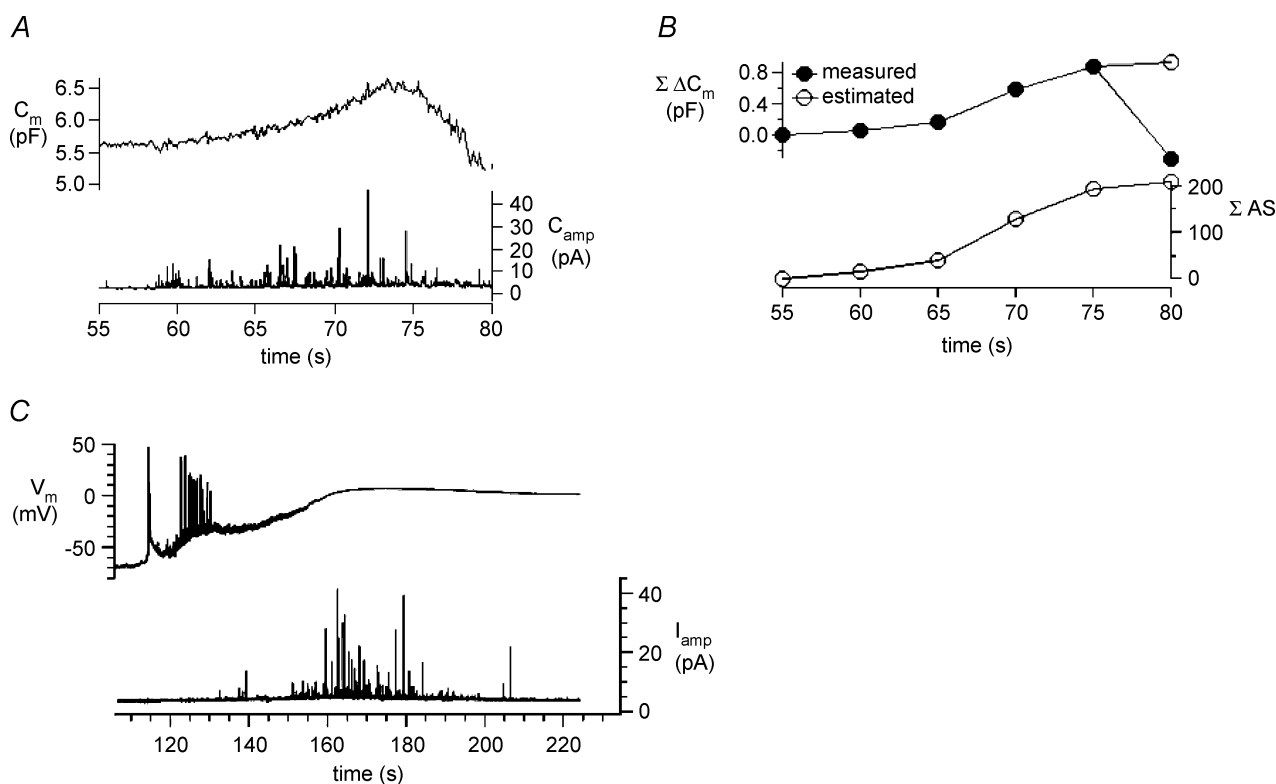
**Figure 6. Examination of the concordance of the various assays of exocytosis in α-LT treated β-cells**
A, displays the exocytotic response to α-LT by a 5-HT-loaded β-cell voltage-clamped at −70 mV, as recorded by simultaneous tracking of C_m (upper trace), and I_{amp} produced by the oxidation of 5-HT release at the cell surface (lower trace). Note that the onsets of both the C_m increase and burst of quantal spikes in the I_{amp} trace begin 58 s after application of α-LT. *B*, displays the similar time course of development of ΔC_m and accumulation of amperometric events (ΣAS) over the 20 s after the onset of exocytosis. Thereafter, the subsequent precipitous drop in C_m, accompanying by persistence of amperometric events, indicates that rapid endocytosis overwhelms slower exocytosis. *C*, simultaneous monitoring of V_m and I_{amp} in response to α-LT in a 5-HT-loaded β-cell current clamped with a holding current of −5 pA. Beginning at 80 s after application of α-LT (at a final concentration of 5 nM) the cell depolarized from −70 mV and fired a barrage of action potentials before settling at a plateau potential of −30 mV where several amperometric events were discharged. Thereafter, the cell further depolarized to a prolonged plateau at ∼0 mV. A massive barrage of amperometric events accompanied the approach to, and maintenance of, the plateau depolarization. *A–C*, β-cells were bathed with 2 mM Ca²⁺ PSS, which contains 2 mM glucose.

to 10 mM or adding 20 μM tolbutamide, a hypoglycaemic sulphonylurea, to the bath each causes a 3- to 7-fold decrease in G_m while producing a similar pattern of initial action potential barrage and subsequent plateau depolarization (Pressel & Misler, 1994). These results suggest that, in contrast to the glucose and sulphonylureas, which close ATP-sensitive K^+ channel(s) that have an equilibrium potential (E_{rev}) negative to -70 mV, the toxin opens a non-selective cation channel with an E_{rev} near 0 mV.

Ion channels induced by α-LT are generally selective to metallic cations and are permeated as well as blocked by Ca^{2+}

The data we have presented thus far suggest that ion channels induced in β-cells by α-LT might be (i) generally cation selective and (ii) blocked as well as permeated by extracellular Ca^{2+}. We designed experiments to test these hypotheses directly in canine β-cells.

In Fig. 7*A*, typical of three experiments, ramps of voltage (from -100 mV to $+60$ mV) were applied to a cell patch clamped with a pipette filled with standard K^+-IS and bathed in standard PSS (2 mM Ca^{2+} PSS) at intervals prior to as well as during the induction of membrane currents by α-LT. This was done to determine the change in shape of the membrane current–voltage (I_m–V_m) relationship associated with α-LT action. Note that prior to the application of α-LT the leak-subtracted I_m changed in a highly non-linear fashion with voltage and consisted of a voltage-activated inward current peaking at $\sim$0 mV and a voltage-activated outward current most prominent at positive voltages (Fig. 7*A*, left traces). In contrast, after α-LT application, a large, inward background current developed at the holding potential of -70 mV, and the current seen during the voltage ramp became almost linear and had a reversal potential near 0 mV (Fig. 7*A*, right traces). The post-toxin current remained nearly ohmic and reversed at 0 mV even when toxin was applied in two other conditions: (i) after blockade of the vast majority
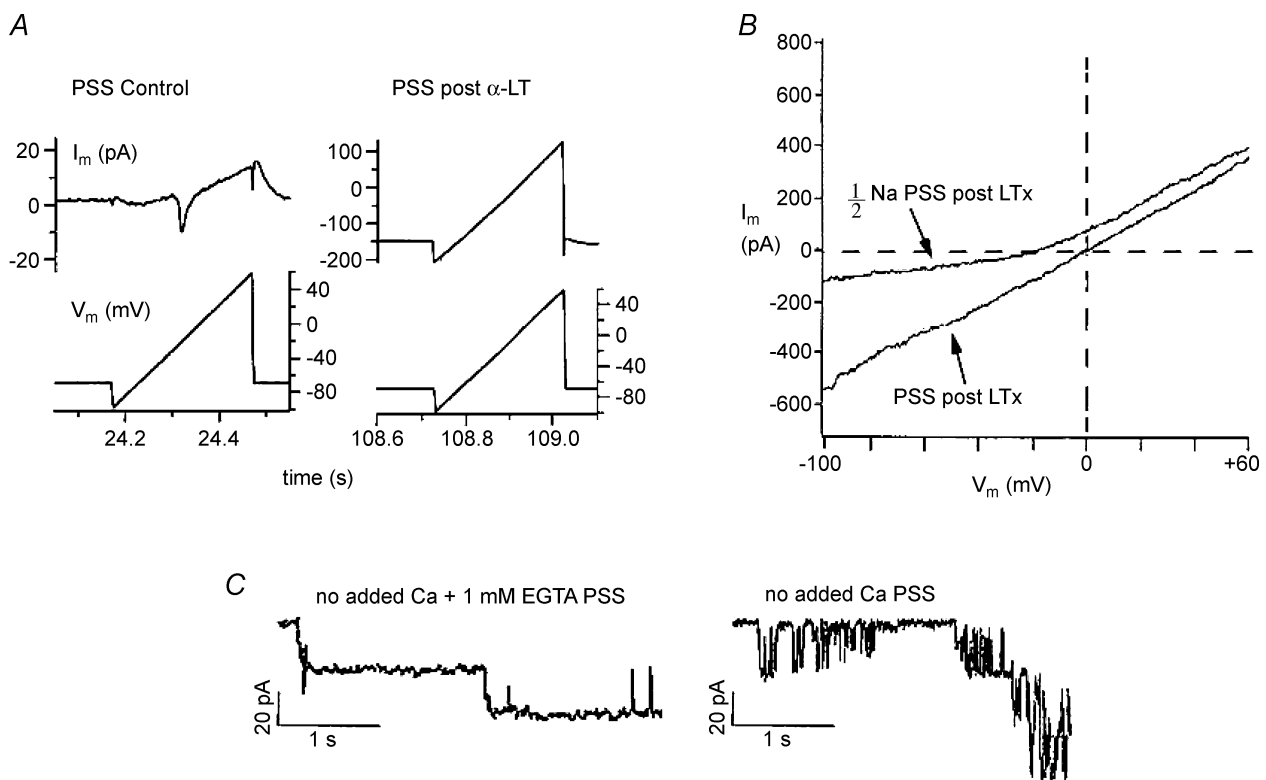
Figure 7. Ionic dependence of currents induced by α-LT in voltage-clamped canine β-cells
A, compares the I_m–V_m relationship of a cell before *versus* after application of 5 nM α-LT in 2 mM Ca^{2+} PSS. The cell was patch clamped with a pipette filled with standard K^+-IS. In each case I_m was recorded in response to 250-ms voltage ramps from -100 mV to $+60$ mV (details in the text). *B*, effect of $[Na^+]_o$ reduction on the I_m–V_m relationship of the toxin-treated cell. When half of the extracellular [NaCl] was replaced with *N*-methyl-D-glucamine (NMDG) chloride, the zero current potential of the cell is shifted negatively by 15 mV and the I_m–V_m relationship shows outward rectification (1/2Na PSS, post α-LT), as compared with the that recorded in 2 mM Ca^{2+} (PSS, post α-LT). *C*, compares single-channel currents recorded from a toxin-treated cell bathed in no added Ca^{2+} PSS (right trace) with those from a toxin-treated cell bathed in no added Ca^{2+}/EGTA PSS (left trace).

of voltage-dependent Na^+ and Ca^{2+} channels in β-cells by addition of 1 μM tetrodotoxin and 50 μM nifedipine to the 2 mM Ca^{2+} PSS; and (ii) in cells patched with Cs^+-IS pipette to block voltage-dependent K^+ channels (data not shown). These results suggested that development of toxin-induced channel activity did not require functional voltage-dependent channels and that the action of α-LT probably blocked gating of voltage-dependent channel, perhaps by causing a sustained rise in $[Ca^{2+}]_i$.

In Fig. 7B, after development of the ohmic toxin-induced current, the bath solution was changed from a standard 2 mM Ca^{2+} PSS to a modified one in which half of the NaCl was replaced isosmotically by the chloride salt of N-methyl-D-glucamine, a large bulky organic cation that poorly permeates non-selective cation channels. This manoeuvre caused the I_m-V_m relationship to display outward rectification and shifted its E_{rev} negatively by 15 mV in this cell (and, an average of 15.8 ± 0.6 mV in three different cells). These results are consistent with toxin-induced current flow through a channel that is almost exclusively cation selective, but poorly selective between Na^+ and K^+.

In Fig. 7C, the onset of development of channel activity was compared under two conditions: (i) toxin-treated cells bathed in no added Ca^{2+}/EGTA PSS (Fig. 7C, left trace), where the estimated concentration of free Ca^{2+} was less than 1 μM; and (ii) similarly treated cells bathed in no added Ca^{2+} + no EGTA PSS (Fig. 7C, right trace), where the estimated concentration of free Ca^{2+} was 5–10 μM. Note that a free extracellular Ca^{2+} concentration of 5–10 μM, estimated to be present in the absence of EGTA, was sufficient to induce rapid flickering in the single channel events as well as subconductance states of channel events.

An additional variable action of α-LT: small concentrations of α-LT that induce little channel activity nevertheless increase depolarization-evoked exocytosis

In our original set of experiments with canine islet cells we noted that not all cells bathed in standard 2 mM Ca^{2+} PSS responded to application of 2–3 nM α-LT with sustained channel activity or detectable 'spontaneous' exocytosis. Also, in these five apparent 'non-responder' cells, application of α-LT did not block depolarization-evoked release, a third effect seen during vigorous response to α-LT. Rather, as illustrated by the example in Fig. 8, in four out of five cells the ΔC_m evoked by a train of depolarizing pulses increased on average 2.4 ± 0.2-fold within 5 min after α-LT application (compare upper traces in Fig. 8A and C), while in
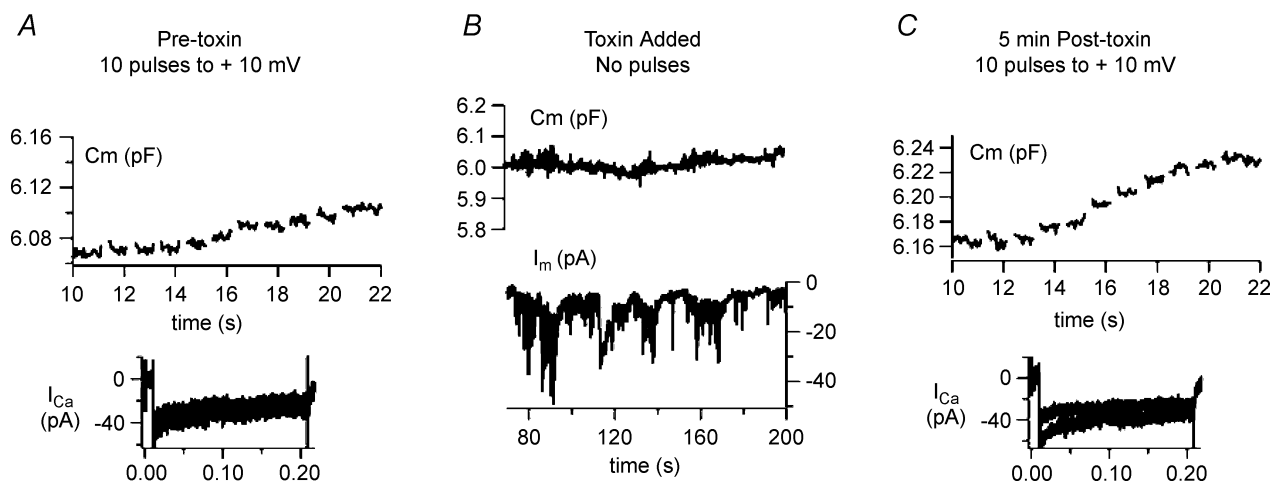
Figure 8. α-LT enhances depolarization-induced exocytosis when it produces rare channel openings and no detectable background exocytosis

A, upper trace shows a representative increase in C_m of canine β-cell bathed in standard PSS in response to a train of ten 200-ms depolarizing pulses to +10 mV (top), from a V_h of −70 mV. The lower traces depict the first and tenth depolarization-induced calcium current (I_{Ca}) recorded during the train. B, upper trace shows that 5 min after addition of 2–3 nM α-LT, the same cell displays a 2-fold larger increase in ΔC_m in response to the train of depolarizations (applied as in A). However, the lower traces demonstrate that the peak amplitude of the first and tenth I_{Ca} recorded during this train differed by less than 10% from those in the initial train shown in A. Note that the resting C_m has changed at most by 80 fF over 5 min. This change is at the limit of the reliability of our capacitance recording system, because with perforated patch recording after repetitive stimulation access resistance can easily change by 1–2 MΩ over 5 min even under the best conditions. C, shows continuous low-gain recordings of C_m (upper trace) and background I_m (lower trace) for the majority of the time interval between addition of α-LT and retesting of depolarization-evoked exocytosis. Note that over this interval C_m varied at most by 100 pF and intermittent channel activity was 40 pA in amplitude.

three out of five cells the depolarization-evoked ΔC_m increased on average 3.6 ± 0.4-fold above control over the next 10–15 min. Enhancement of evoked release occurred either (i) in the absence of an increase in peak voltage-dependent Ca^{2+} current (I_{Ca}) (compare lower traces in Fig. 8*A* and *C*) or in the total Ca^{2+} charge entry, Q_{Ca} (i.e. integral of the total Ca^{2+} current) or (ii) in the presence of a 24% decline in Q_{Ca}, as seen in two cells. In contrast, in control cells not treated with α-LT, typically there was a progressive $31 \pm 8\%$ decline in C_m with repeated trains of depolarization accompanied by only an $8.3 \pm 2\%$ decline in Q_{Ca}.

A priori, a variety of basic mechanisms might underlie the toxin's ability to enhance depolarization-evoked quantal release in the absence of an increase in voltage-dependent Ca^{2+} entry. For example, intermittent bursts of Ca^{2+} entry through toxin-induced channels might raise the background cytosolic Ca^{2+} concentration to levels that increase the readily releasable pool (RRP) of granules. Alternatively, toxin bound to its receptor might activate another intracellular second messenger that increases the RRP or alters the time course of regulation of cytosolic Ca^{2+}. To evaluate these possibilities, we performed repetitive depolarization experiments on Fura-2 -loaded cells before and after application of low doses of α-LT.

Figure 9 shows the two patterns of augmentation of depolarization-evoked exocytosis caused by application of 600 pM α-LT. In four out of seven experiments (see Fig. 9*A* for representative experiment), the total increase in membrane capacitance ($\Sigma C_{m,step}$) seen during the tetanus (five 200-ms depolarizations to $+10$ mV at 1-s intervals) as well as the slower, creeping increase in membrane

capacitance ($\Delta C_{m,creep}$) seen at the end of the tetanus were enhanced by 1.75 ± 0.15-fold and 2.7 ± 0.2-fold, respectively, 5 min after application of α-LT (compare pre-toxin and post-toxin traces). However, baseline $[Ca^{2+}]_i$, the $C_{m,step}$ in response to the initial 200-ms depolarization, as well as the time course of the intra-tetanic rise in $[Ca^{2+}]_i$ and subsequent decay of $[Ca^{2+}]_i$ all changed by $< 10\%$. This result is consistent with an increase in the number of release-ready insulin granules (or the Ca^{2+} sensitivity of these granules), perhaps by the generation of a non-Ca^{2+}-dependent second messenger. In contrast, in the remaining three experiments (see Fig. 9*B* for representative experiment), application of α-LT resulted in enhancement of the rise in $[Ca^{2+}]_i$ during the depolarizing tetanus as well as a reduction in the rate of decline thereafter. In these cells $\Sigma C_{m,step}$ and $\Delta C_{m,creep}$ were each increased on average by 3.5 ± 0.25-fold and even $C_{m,step}$ in response to the initial 200-ms depolarization was enhanced on average by 2.05 ± 0.08-fold. This result suggests that under some circumstances α-LT might modulate processes of cytosolic Ca^{2+} homeostasis.

Discussion

α-LT, probably operating through several mechanisms, is a potent secretagogue for a variety of excitable endocrine cells containing large dense core secretory granules, as well as for neurones containing smaller synaptic vesicles (Südhof, 2001). The toxin-sensitive endocrine cells include catecholamine-secreting adrenal medullary chromaffin cells (Barnett *et al.* 1996; Bittner *et al.* 1998), follicle-stimulating hormone- and luteinizing hormone-secreting pituitary gonadotropes (Tse & Tse,
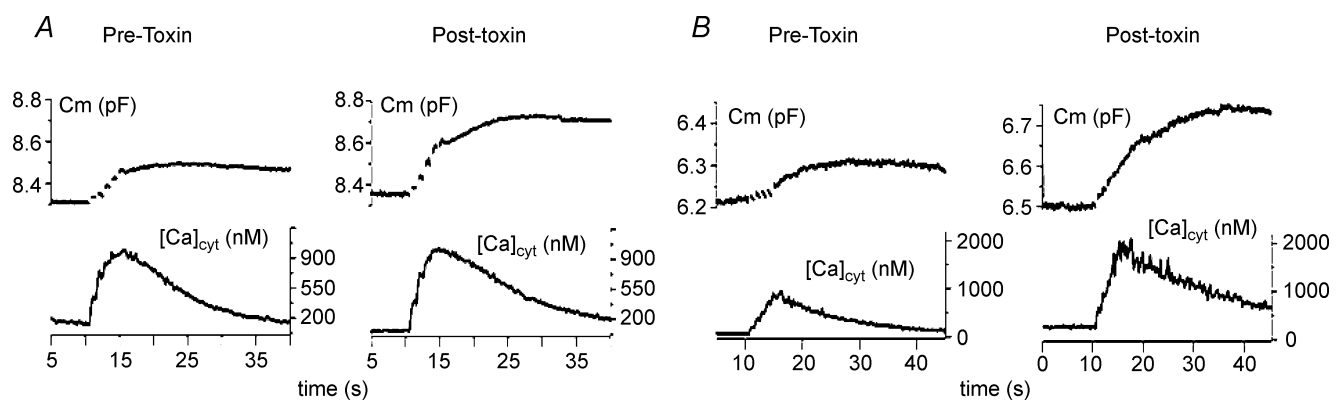
Figure 9. Two patterns of augmentation of depolarization-evoked exocytosis produced by low-dose (600 pm) α-LT
Simultaneous recording of C_m (upper trace) and $[Ca^{2+}]_i$ (lower trace) from Fura-2-loaded β-cells patch clamped at a V_h of -70 mV. *A*, the C_m response to a depolarizing train (five 200-ms long pulses to $+10$ mV applied at 1 Hz) increased from a control value (Pre-α-LT) of 215 fF to 420 fF by 5 min after addition of 600 pm α-LT (Post-α-LT) but was not accompanied by a change in the amplitude or time course of the $[Ca^{2+}]_i$ enhancement. *B*, C_m response to an identical depolarizing train increased from a control value (Pre-α-LT) of 80 fF to 250 fF by 5 min after addition of 600 pm α-LT (Post-α-LT). Note that this was accompanied by doubling of the enhancement of $[Ca^{2+}]_i$ amplitude during the depolarizing train as well as the duration of $[Ca^{2+}]_i$ enhancement both during and after stimulation.

1999) and native or clonal insulin-secreting cells derived from pancreatic islets of Langerhans (Lang *et al.* 1998). We have investigated the action of α-LT on single insulin-secreting β-cells obtained from human, canine and mouse pancreatic islets of Langerhans using two single-cell electrophysiological assays of exocytosis, namely capacitance measurements (Gillis & Misler, 1992; Ammala *et al.* 1993) and amperometry (Smith *et al.* 1995; Zhou & Misler, 1995; Huang *et al.* 1995), as well as fluorescence imaging of cytosolic Ca^{2+} concentration. Our results confirm those of a previous report (Lang *et al.* 1998) that α-LT enhances exocytosis from both resting and stimulated β-cells. However, our results point to different mechanisms of action than that proposed in the prior report. Lang *et al.* (1998) presented evidence that α-LT, applied at nanomolar concentrations, produces 2- to 3-fold enhancements of insulin secretion in both the presence and absence of extracellular Ca^{2+}, as well as in the absence of the ability of α-LT to form ion channels in the plasma membrane or raise cytosolic Ca^{2+} concentration. On this basis, they proposed that the major effect of α-LT is via a receptor-mediated second messenger pathway operating independently of, or at a fixed baseline level of cytosolic Ca^{2+}.

In our experiments performed on 'resting' β-cells (i.e. held at their resting potential or bathed in sub-stimulatory concentrations of glucose), the secretagoue action of α-LT is closely linked to the formation of large conductance, cation-selective plasma membrane channels, through which extracellular Ca^{2+} enters the cytoplasm, accumulates and then triggers the fusion of secretory granules with the plasma membrane. The toxin-induced channels we observe in β-cells are very similar to those seen in patch-clamped pituitary gonadotropes, neurohypophysial terminals and chromaffin cells. As in the latter cell types (Dunn & Holz, 1983; Augustine & Neher, 1992), in β-cells global cyto-solic Ca^{2+} concentration must rise to > 500–600 nM to support enhanced exocytosis (Jones *et al.* 1992; Ammala *et al.* 1993). This also applies after application of α-LT: as the cytosolic Ca^{2+} concentration rises above ~ 500 nM, the rate of exocytosis increases by many hundred-fold from < 0.01 granules s^{-1} to > 100 granules s^{-1}. We shall refer to this proposed mechanism of α-LT action as 'channel formation/Ca^{2+} entry'.

In our experiments with 'stimulated' β-cells (i.e. those depolarized to evoke voltage-dependent Ca^{2+} currents), we demonstrate that smaller, subnanomolar doses of α-LT can enhance depolarization-evoked exocytosis several-fold, regardless of whether it induces background channel activity or enhances cytosolic $[Ca^{2+}]$. This latter action was previously reported with adrenal chromaffin cells (Liu & Misler, 1998). In cells where background and depolarization-evoked levels of cytosolic $[Ca^{2+}]$ are unchanged by α-LT, we propose that α-LT is increasing

insulin granule release either by increasing the size of a pool of releasable granules or by increasing its Ca^{2+} sensitivity. This might occur by receptor-mediated activation of a second-messenger system or by inter-action with the exocytotic apparatus (Petrenko *et al.* 1991). We shall refer to this mechanism of toxin action as 'granule recruitment'. Currently, there is no direct evidence concerning whether or which second messengers might underlie such an effect in β-cells, though evidence from chromaffin cells, pretreated with a plasma-permeabilizing membrane detergent, suggests that activation of protein kinase C (PKC) might play a role (Bittner & Holz, 2000).

It is likely that the 'channel formation/Ca^{2+} entry' and 'granule recruitment' actions are often complementary. As the channel-independent effect of toxin occurs at lower doses than the channel forming effect, it might contribute significantly to the massive secretory effect seen in the presence of channel formation. We have obtained some evidence for this channel-independent effect in the presence of channel activity. In three experiments, we compared the rates of exocytosis seen after repetitive depolarization in the absence of α-LT with the rates of exocytosis subsequently seen in response to channel-forming doses of α-LT in the absence of depolarization (see Fig. 8). At similar levels of slowly changing global levels of $[Ca^{2+}]_i$, presumed to be well equilibrated over the entire volume of cytoplasm, rates of exocytosis were on average 3.2-fold higher in the presence *versus* the absence of toxin. (However, as this effect is not evident in the absence of a rise in $[Ca^{2+}]_i$, it is not clear how it relates to the Ca^{2+}-independent effect of toxin seen by Lang *et al.* (1998), or the Ca^{2+}-independent effect of toxin widely reported at nerve terminals). On the other hand, low doses of α-LT present for many minutes can produce brief bursts of channel activity that are likely to underlie transient, submicromolar level increases in $[Ca^{2+}]_i$ which in turn can 'prime' later depolarization-induced exocytosis in endocrine cells (e.g. Von Ruden & Neher, 1993; Misler, 2003). Hence, brief Ca^{2+} entry through toxin-induced channels may bolster granule recruitment.

In the case of either mechanism (channel formation/Ca^{2+} entry or granule recruitment), a likely, and experimentally testable, candidate for a pool of granules that heavily contributes to toxin-induced exocytosis is a highly Ca^{2+}-sensitive pool (HCSP). This pool, newly described in chromaffin and β-cells (Yang *et al.* 2002; Yang & Gillis, 2004; Wan *et al.* 2004) largely through the use of flash photolysis of caged Ca^{2+} compounds to rapidly raise global cytosolic $[Ca^{2+}]$, consists of granules released by rises in $[Ca^{2+}]_i$ between $< 1 \mu$M and $\sim 10 \mu$M. The HCSP does not appear to be highly colocalized with voltage-dependent Ca^{2+} channels in that it contributes little to the immediate release of quanta after a very brief (duration, 5–10 ms) action potential-like depolarization. It is also enhanced

by augmentation of cytosolic PKC activity. Moreover, the HCSP appears to contribute significantly to the asynchronous release seen after prolonged or repeated depolarizations, for example, the creep-wise increase in C_m and the tail of amperometric events continuing as long as several seconds after completion of a train of 100- to 200-ms depolarizations.

In our work (this paper as well as Liu & Misler, 1998) we have described several aspects of toxin-related enhancement of exocytosis in endocrine cells that occur at $[Ca^{2+}]_i > 500$ nM, comparable to the cytosolic Ca^{2+} threshold for release from the HCSPs of these cells. These aspects are: (i) toxin-induced exocytosis during vigorous toxin-induced channel activity and rise in $[Ca^{2+}]_i$; and (ii) toxin-induced enhancement of the total C_m increase during a train of depolarizations as well as the subsequent ΔC_m tail after a train in the absence of toxin-induced channel activity. Hence we propose that the HCSP is the major pool utilized in toxin action. Examination of the size, dynamics and Ca^{2+} sensitivity of insulin granule pools using flash photolysis of caged Ca^{2+} compounds will be needed to provide a more direct test of this hypothesis. Newly engineered toxin molecules that have little channel-forming ability (Volynski *et al.* 2003) may be particularly useful in this regard.

Though we have not reported direct measurements of insulin secretion in this single-cell study, it is very likely that our experimental assay of exocytosis truly reflects insulin release. First, in our pilot experiments on the effects of α-LT on perifused human islets, we found that over 20 min following its administration, 2 nM α-LT enhanced insulin release, in 3 mM glucose, a non-stimulatory glucose concentration, on average 12-fold in the presence, but not in the absence, of physiological $[Ca^{2+}]_o$ (S. Boyle and S. Misler, unpublished data). This occurred despite an anticipated slow penetration of islets by the large molecular weight toxin. Second, in amperometric experiments where single-cell quantal release of 5-HT and insulin were measured simultaneously with separate carbon fibre electrodes, secretagogue stimuli such as KCl produced parallel increases in both assays of exocytosis (Huang *et al.* 1995).

Our results with β-cells support the hypothesis that α-LT binds to one or more plasma membrane receptors, and then inserts itself into the plasma membrane, where it partially translocates, thereby becoming resistant to proteolysis (Südhof, 2001). At low doses of α-LT, the translocation of small numbers of α-LT molecules may allow them (i) to interact with Soluble *N*-ethylmaleimide-sensitive factor attachment protein receptor (SNARE) proteins of the exocytotic apparatus and release the restraint on $[Ca^{2+}]_i$-dependent release (Bittner *et al.* 1998) or (ii) to enhance the ability of the cytoplasmic domain of the toxin receptors to interact with a G-protein. This may account for the toxin's ability to enhance depolarization-induced quantal release. At higher doses of α-LT, translocated segments of toxin monomers may aggregate to form Ca^{2+}-permeable channels, perhaps in a way similar to the oligomerization of toxin molecules in solution (Orlova *et al.* 2000). This may account for the toxin's ability to support Ca^{2+} entry, increase cytosolic $[Ca^{2+}]$ and $[Ca^{2+}]_i$-dependent exocytosis. These two actions are identical to those we have previously reported in adrenal medullary chromaffin cells (Liu & Misler, 1998) and parallel the original observations of the actions of crude black widow spider venom at neuromuscular junctions bathed in a physiological saline solution (Longenecker *et al.* 1970). At the concentrations of toxin we used, and within the limits of our assays, we found no evidence for any of the following: (i) large or sustained release of Ca^{2+} from intracellular stores that would detectably raise global cytosolic $[Ca^{2+}]$; (ii) non-exocytotic release of the measured transmitter 5-HT as reflected by major cell swelling or cell lysis that might contribute to non-exocytotic release of granules or non-quantal increases in amperometric current; or (iii) obvious alterations in the kinetics of the fusion pore mechanism, as manifested by changes in the configuration of the foot or fast upstroke of amperometric spike events.

Previous studies with clonal β-cell lines (Lang *et al.* 1998) suggest that one or more $[Ca^{2+}]_o$-independent receptor(s) of α-LT (CIRL/latrophilin or CL) may participate. We have no independent biochemical evidence regarding the structure of α-LT receptor(s) responsible for its actions in human, canine and murine β-cells. However, our experiments (see Figs 1 and 3) indicate that the toxin can be applied to β-cells, and then vigorously washed away, in the presence of no added Ca^{2+}_o and 1–5 mM EGTA, and still produce characteristic channel activity, a rise in cytosolic $[Ca^{2+}]$ and quantal release after re-addition to the bath of Ca^{2+} at millimolar concentrations. These results are consistent with some isoform of CIRL/latrophilin playing a major role in toxin binding. The 10- to 15-fold higher concentration of toxin needed to produce exocytosis in β-cells *versus* neurones suggests that the toxin receptors in β-cells may be a lower affinity variant of CL (for example, CL-2 rather than the high affinity brain-type variant CL-1; Ichtchenko *et al.* 1999), or may be present at significantly lower density.

References

Ammala C, Eliasson L, Bokvist K, Larsson O, Ashcroft FM & Rorsman P (1993). Exocytosis elicited by action potentials and voltage-clamp calcium currents in individual mouse pancreatic B-cells. *J Physiol* **472**, 665–688.

Ashton AC, Volynski KE, Lelianova VG, Orlova EV, Van Renterghem C, Canepari M, Seagar M & Ushkaryov YA (2001). alpha-Latrotoxin, acting via two Ca^{2+}-dependent pathways, triggers exocytosis of two pools of synaptic vesicles. *J Biol Chem* **276**, 44695–44703.

Augustine GJ & Neher E (1992). Calcium requirements for secretion in bovine chromaffin cells. *J Physiol* **450**, 247–271.

Barnett DW, Liu J & Misler S (1996). Single-cell measurements of quantal secretion induced by alpha-latrotoxin from rat adrenal chromaffin cells: dependence on extracellular Ca^{2+}. *Pflugers Arch* **432**, 1039–1046.

Barnett DW & Misler S (1997). An optimized approach to membrane capacitance estimation using dual-frequency excitation. *Biophys J* **72**, 1641–1658.

Barnett DW, Pressel DM, Chern HT, Scharp DW & Misler S (1994). cAMP-enhancing agents 'permit' stimulus-secretion coupling in canine pancreatic islet β-cells. *J Membr Biol* **138**, 113–120.

Bittner MA & Holz RW (2000). Latrotoxin stimulates secretion in permeabilized cells by regulating an intracellular Ca^{2+}- and ATP-dependent event: a role for protein kinase C. *J Biol Chem* **275**, 25351–25357.

Bittner MA, Krasnoperov VG, Stuenkel EL, Petrenko AG & Holz RW (1998). A Ca^{2+}-independent receptor for alpha-latrotoxin, CIRL, mediates effects on secretion via multiple mechanisms. *J Neurosci* **18**, 2914–2922.

Bruns D & Jahn R (1995). Real-time measurement of transmitter release from single synaptic vesicles. *Nature* **377**, 62–65.

Davletov BA, Shamotienko OG, Lelianova VG, Grishkin EV & Ushkaryov YA (1996). Isolation and biochemical characterization of a Ca^{2+}-independent alpha-latrotoxin binding protein. *J Biol Chem* **271**, 23239–23245.

Dunn LA & Holz RW (1983). Catecholamine secretion from digitonin-treated adrenal medullary chromaffin cells. *J Biol Chem* **258**, 4989–4993.

Finkelstein A, Rubin LL & Tzeng MC (1976). Black widow spider venom: effect of purified toxin on lipid bilayer membranes. *Science* **193**, 1009–1011.

Gillis KD & Misler S (1992). Single cell assay of exocytosis from pancreatic islet B cells. *Pflugers Arch* **420**, 121–123.

Gopel S, Kanno T, Barg S, Galvanovskis J & Rorsman P (1999). Voltage-gated and resting membrane currents recorded from β-cells in intact mouse pancreatic islets. *J Physiol* **521**, 717–728.

Grynkiewicz G, Poenie M & Tsien RY (1985). A new generation of Ca^{2+} indicators with greatly improved fluorescence properties. *J Biol Chem* **260**, 3440–3450.

Hlubek MD, Stuenkel EL, Krasnoperov VG, Petrenko AG & Holz RW (2000). Calcium-independent receptor for alpha-latrotoxin and neurexin 1 alpha facilitate toxin-induced channel formation. *Mol Pharm* **57**, 519–528.

Hlubek M, Tian D & Stuenkel EL (2003). Mechanisms of α-latrotoxin action at nerve endings of neurohypophysis. *Brain Res* **992**, 30–42.

Huang L, Shen H, Atkinson MA & Kennedy RT (1995). Detection of exocytosis at individual pancreatic β-cells by amperometry at a chemically modified microelectrode. *Proc Natl Acad Sci U S A* **92**, 398–404.

Hurlbut WP, Chieregatti E, Valtorta F & Haimann C (1994). Alpha-latrotoxin channels in neuroblastoma cells. *J Membr Biol* **138**, 91–102.

Ichtchenko K, Bittner MA, Krasnoperov V, Little AR, Chepurny O, Holz RW & Petrenko AG (1999). A novel ubiquitously expressed alpha-latrotoxin receptor is a member of the CIRL family of G-protein-coupled receptors. *J Biol Chem* **274**, 5491–5498.

Jones PM, Persaud SJ & Howell SL (1992). Ca^{2+}-induced insulin secretion from electrically permeabilized islets. Loss of the Ca^{2+}-induced secretory response is accompanied by loss of Ca^{2+}-induced protein phosphorylation. *Biochem J* **285**, 973–978.

Krasnoperov VG, Bittner MA, Beavis R, Kuang Y, Salnikow KV, Chepurny OG, Little AR, Plotnikov AN, Wu D, Holz RW & Petrenko AG (1997). alpha-Latrotoxin stimulates exocytosis by the interaction with a neuronal G-protein-coupled receptor. *Neuron* **18**, 925–937.

Krasnoperov V, Bittner MA, Mo W, Buryanovsky L, Neubert TA, Holz RW, Ichtchenko K & Petrenko AG (2002). Protein-tyrosine phosphatase-sigma is a novel member of the functional family of alpha-latrotoxin receptors. *J Biol Chem* **277**, 35887–35895.

Lacy PE & Kostianovsky M (1967). Method for the isolation of intact islet of Langerhans from the rat pancreas. *Diabetes* **16**, 35–39.

Lang J, Ushkaryov Y, Grasso A & Wollheim CB (1998). Ca^{2+}-independent insulin exocytosis induced by alpha-latrotoxin requires latrophilin, a G protein-coupled receptor. *EMBO J* **17**, 648–657.

Liu J & Misler S (1998). alpha-latrotoxin alters spontaneous and depolarization-evoked quantal release from rat adrenal chromaffin cells: evidence for multiple modes of action. *J Neurosci* **18**, 6113–6125.

Liu-Gentry J, Silva AM, Barnett DW & Misler S (2004). alpha-latrotoxin: a potent dual mode enhancer of β-cell exocytosis. *Diabetes* **53**, A583.

Longenecker HE Jr, Hurlbut WP, Mauro A & Clark AW (1970). Effects of black widow spider venom on the frog neuromuscular junction. Effects on end-plate potential, miniature end-plate potential and nerve terminal spike. *Nature* **225**, 701–703.

Meldolesi J, Huttner WB, Tsien RB & Pozzan T (1984). Free cytoplasmic Ca^{2+} and neurotransmitter release: studies on the PC12 cells and synaptosomes exposed to alpha-latrotoxin. *Proc Natl Acad Sci U S A* **81**, 620–624.

Misler S (2003). Delayed and sustained depolarization-evoked exocytosis in B cells of large mammals. *Diabetes* **52**, A2.

Misler S & Hurlbut WP (1979). Action of black widow spider venom on quantal release of acetylcholine at the frog neuromuscular junction: dependence upon external Mg^{2+}. *Proc Natl Acad Sci U S A* **76**, 991–995.

Missler M, Hammer RE & Südhof TC (1998). Neurexophilin binding to α-neurexins. A single LNS domain functions as an independently folding ligand-binding unit. *J Biol Chem* **273**, 34716–34723.

Okamoto M, Longenecker HE Jr, Riker WF Jr & Song SK (1971). Destruction of mammalian motor nerve terminals by black widow spider venom. *Science* **172**, 733–736.

Orlova EV, Rahman MA, Gowen B, Volynski KE, Ashton AC, Manser C, van Heel M & Ushkaryov YA (2000). Structure of alpha-latrotoxin oligomers reveals that divalent cation-dependent tetramers form membrane pores. *Nat Struct Biol* **7**, 48–53.

Petrenko AG, Perin MS, Davletov BA, Ushkaryov YA, Geppert M & Sudhof TC (1991). Binding of synaptotagmin to the alpha-latrotoxin receptor implicates both in synaptic vesicle exocytosis. *Nature* **353**, 65–68.

Pipeleers DG & Van de Winkel M (1987). Separation of pancreatic islet cells according to functional characteristics. In *Cell Separation: Methods and Selected Applications*, Pretlow TG, pp. 119–140. Academic Press, Orlando.

Pressel DM & Misler S (1994). Role of voltage-depedent ionic currents in coupling glucose stimulation to insulin secretion in canine pancreatic islet B-cells. *J Membr Biol* **124**, 239–253.

Ricordi C, Lacy PE, Finke EH, Olack BJ & Scharp DW (1988). Automated method for isolation of human pancreatic islets. *Diabetes* **37**, 413–420.

Rosenthal L, Zacchetti D, Madeddu L & Meldolesi J (1990). Mode of action of alpha-latrotoxin: role of divalent cations in Ca^{2+}- dependent and Ca^{2+}-independent effects mediated by the toxin. *Mol Pharmacol* **38**, 917–923.

Smith PA, Duchen MR & Ashcroft FM (1995). A fluorimetric and amperometric study of calcium and secretion in isolated mouse pancreatic β–cells. *Pflugers Arch* **430**, 808–818.

Südhof TC (2001). alpha-Latrotoxin and its receptors: neurexins and CIRL/latrophilins. *Annu Rev Neurosci* **24**, 933–962.

Tsang CW, Elrick DB & Charlton MP (2000). α-latrotoxin releases calcium in frog motor nerve terminals. *J Neurosci* **20**, 8685–8692.

Tse FW & Tse A (1999). Alpha-latrotoxin stimulates inward current, rise in cytosolic calcium concentration, and exocytosis in rat pituitary gonadotropes. *Endocrinology* **140**, 3025–3033.

Volynski KE, Capogna M, Ashton AC, Thomson D, Orlova EV, Manser CF, Ribchester RR & Ushkaryov YA (2003). Mutant α-latrotoxin (LTX^{N4C}) does not form pores and causes secretion by receptor stimulation. *J Biol Chem* **278**, 31058–31066.

Von Ruden L & Neher E (1993). A Ca-dependent early step in release of catecholamines from adrenal chromaffin cells. *Science* **262**, 1061–1065.

Wan QF, Yang H, Lou X, Ding J & Xu T (2004). Protein kinase activation increases insulin secretion by sensitizing the secretory machinery to Ca^{2+}. *J Gen Physiol* **124**, 653–662.

Yang Y & Gillis KD (2004). A highly Ca^{2+}-sensitve pool of granules is regulated by glucose and protein kinase in insulin-secreting INS-1 cells. *J Gen Physiol* **124**, 641–651.

Yang Y, Udayasankar S, Dunning J, Chen P & Gillis KD (2002). A highly Ca^{2+}-sensitive pool of vesicles is regulated by protein kinase C in adrenal chromaffin cells. *Proc Natl Acad Sci U S A* **99**, 17060–17065.

Zhou Z & Misler S (1995). Amperometric detection of quantal release of serotonin from canine pancreatic islet β-cells. *Abstr Soc Neurosci* **21**, 334.

Zhou Z & Misler S (1996). Amperometric detection of quantal secretion from patch-clamped rat pancreatic β-cells. *J Biol Chem* **271**, 270–277.

Acknowledgements

Authors' present addresses

A. Silva: Department of Biological and Environmental Engineering, CETAV, Universidade de Tras-os-Montes e Alto Douro, Vila Real, Portugal.

A. S. Dickey: Medical Scientist Training Program, University of Chicago Medical Center, Chicago, IL 60637, USA.

Supplemental material

The online version of this paper can be accessed at:
DOI: 10.1113/jphysiol.2005.082586
http://jp.physoc.org/cgi/content/full/jphysiol.2005.082586/DC1
and contains supplemental material consisting of a figure entitled: α-LT enhances radioimmunoassayed insulin and glucagon secretion from glucose-responsive, perifused human islets in a Ca^{2+}_{o}-dependent manner.

This material can also be found as part of the full-text HTML version available from http://www.blackwell-synergy.com